Pteridine reductase mechanism correlates pterin metabolism with drug resistance in trypanosomatid parasites

David G. Gourley[1,2], Alexander W. Schüttelkopf[1,2], Gordon A. Leonard[3], James Luba[4], Larry W. Hardy[4,5], Stephen M. Beverley[6] and William N. Hunter[1]

[1]The Wellcome Trust Biocentre, University of Dundee, Dundee, DD1 5EH, UK. [2]The first two authors contributed equally to this research. [3]Joint Structural Biology Group, ESRF, BP 220, F38043, Grenoble, Cedex 9, France. [4]Department of Pharmacology and Molecular Toxicology, University of Massachusetts Medical School, 373 Plantation St., Worcester, Massachusetts 01605, USA. [5]ArQule Inc., 19 Presidential Way, Woburn, Massachusetts 02154, USA. [6]Department of Molecular Microbiology, Washington University School of Medicine, Campus Box 8230, 660 S. Euclid Avenue, St. Louis, Missouri 63110-1093, USA.

Pteridine reductase (PTR1) is a short-chain reductase (SDR) responsible for the salvage of pterins in parasitic trypanosomatids. PTR1 catalyzes the NADPH-dependent two-step reduction of oxidized pterins to the active tetrahydro-forms and reduces susceptibility to antifolates by alleviating dihydrofolate reductase (DHFR) inhibition. Crystal structures of PTR1 complexed with cofactor and 7,8-dihydrobiopterin (DHB) or methotrexate (MTX) delineate the enzyme mechanism, broad spectrum of activity and inhibition by substrate or an antifolate. PTR1 applies two distinct reductive mechanisms to substrates bound in one orientation. The first reduction uses the generic SDR mechanism, whereas the second shares similarities with the mechanism proposed for DHFR. Both DHB and MTX form extensive hydrogen bonding networks with NADP(H) but differ in the orientation of the pteridine.

The protozoan parasites *Leishmania* and *Trypanosoma* are auxotrophic for folate and other pterins required in critical pathways, including nucleic acid and protein biosynthesis. Thus, these parasites rely on uptake from the host combined with reduction to the active tetrahydro-forms of pterin compounds[1–4]. This suggests that antifolates should serve as useful drugs against diseases caused by parasites, such as African sleeping sickness, Chagas' disease and the leishmaniases. The failure of antifolate drugs to do so is both surprising and disappointing.

Following uptake, pterins, such as biopterin or folate, undergo two successive reductions to yield the active tetrahydro-species. Two enzymes carry out these reactions in trypanosomatids. A bifunctional dihydrofolate reductase-thymidylate synthase (DHFR-TS) is the major enzyme responsible for the reduction of folate and 7,8-dihydrofolate (DHF) to 5,6,7,8-tetrahydrofolate (THF)[4–6]. A second enzyme, PTR1, carries out reductions of conjugated and unconjugated pterins — for example, of biopterin to dihydrobiopterin (DHB) then subsequently to 5,6,7,8-tetrahydrobiopterin (THB)[3,7] or of folate to DHF and THF. PTR1 is the only enzyme known to reduce biopterin in *Leishmania* and has been proven to be essential for growth *in vivo* by gene knockout studies[1,3]. Because PTR1 is less sensitive

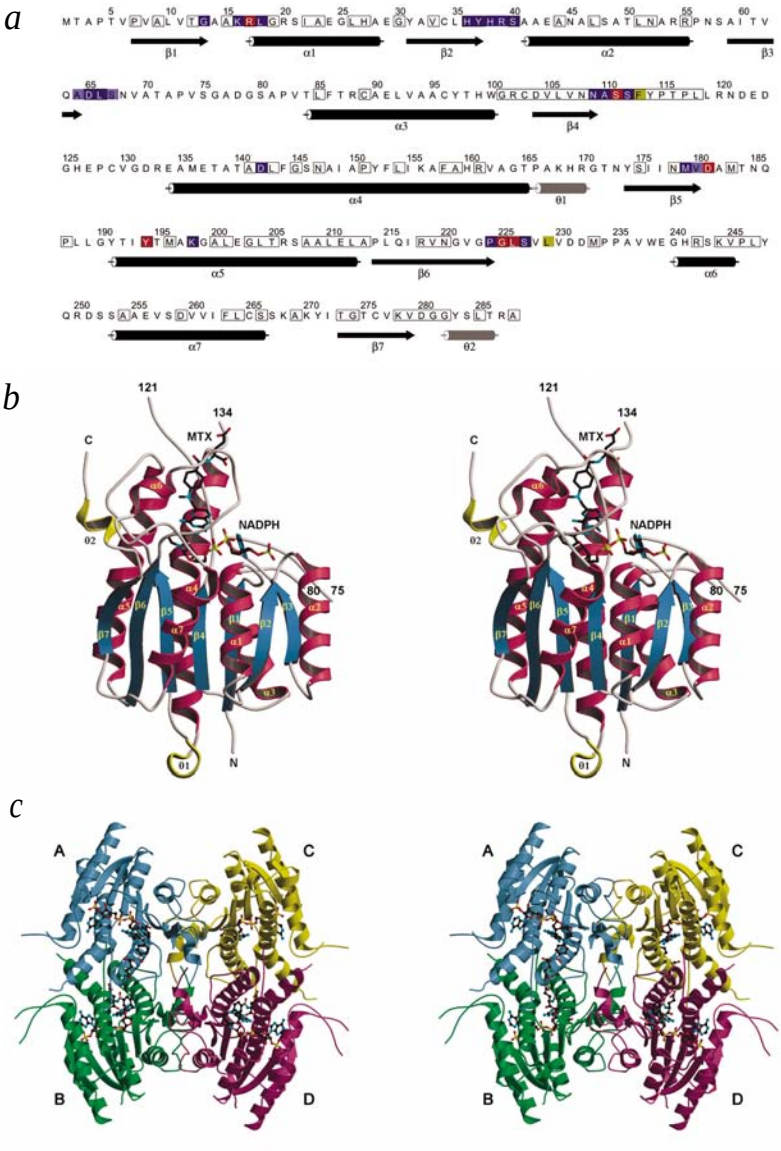

Fig. 1 The sequence and structure of *L. major* PTR1. ***a***, Amino acid sequence and secondary structure assignment. Black and gray cylinders depict α-helices and 3_{10}-helices (θ), respectively. Boxed residues are conserved in available PTR1 sequences. The colored boxes identify residues 4.0 Å or less from cofactor or the DHB substrate. Yellow identifies residues that contact DHB, blue identifies those that contact the cofactor (light blue = main chain only) and red marks residues that contact both. ***b***, Stereo view ribbon diagram of a subunit. The α-helices are purple, 3_{10}-helices are yellow, β-strands are cyan and random coil, gray. MTX and NADPH are stick models colored according to atom type: nitrogen = cyan, carbon = black, oxygen = red and phosphorus = yellow. N- and C-terminal positions are marked, and residue numbers are used to identify chain breaks. ***c***, Stereo view of the functional tetramer. Each subunit is given a different color and labeled A–D.

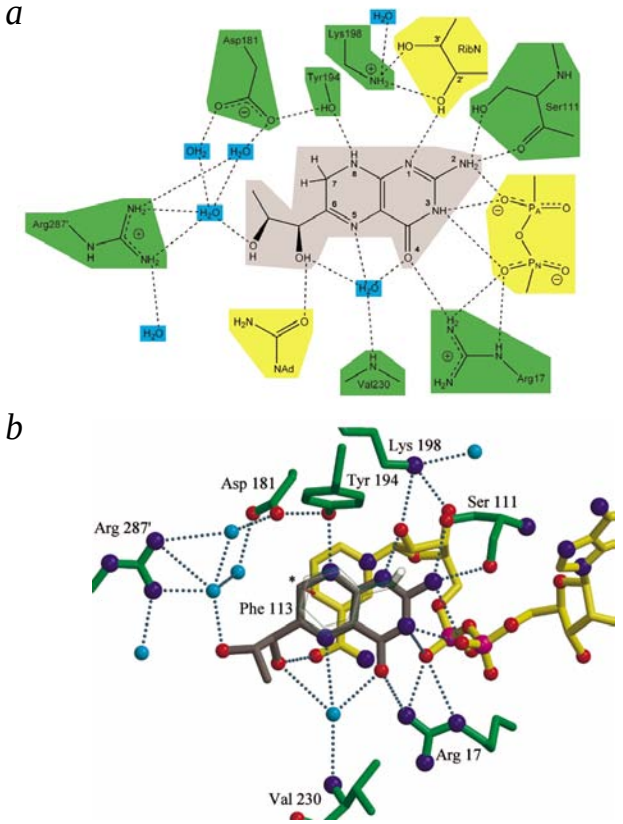

Fig. 2 The interactions of DHB with PTR1 and NADP+. ***a***, Schematic. Dashed lines represent hydrogen bonds of length ≤3.5 Å. ***b***, Three-dimensional arrangement. Atoms are colored as in Fig. 1. The cyan dashed lines represent hydrogen bonds, and the proximity of the nicotinamide C4 and C7 of substrate DHB (asterisked), required for the first hydride transfer, is indicated by a red dashed line. Phe 113 has been ghosted for clarity.

to methotrexate (MTX) than DHFR (IC_{50} = 1.1 μM and 0.005 μM for *L. major* PTR1 and DHFR-TS, respectively)[1,5] but catalyzes the reduction of DHF, it compromises drugs targeting DHFR by acting as a metabolic bypass[3]. This, in part, explains why antifolate therapies have failed against trypanosomatid infections[4,6,8].

To investigate the molecular basis of antifolate resistance, we determined the crystal structures of PTR1–NADP+–DHB and PTR1–NADPH–MTX complexes. The structures provide details of protein–pterin interactions, the mechanism, modes of inhibition and the structural basis for the broad substrate specificity of the enzyme.

Architecture of PTR1

The 288-residue PTR1 polypeptide forms a single α/β domain with typical short-chain reductase (SDR) topology based on the Rossmann fold: a seven-stranded parallel β-sheet sandwiched between three helices on either side[9–11] (Fig. 1*a*,*b*). The catalytic center is mainly constructed from a single chain using residues at the C-terminal regions of β1, β4, β5 and β6; the N-terminal sections of α1 and α5; and the loop between β6 and α6.

The functional enzyme is a tetramer (subunits A, B, C and D) with 222-point group symmetry; however, there is no evidence for cooperativity in the mechanism. Because of the assembly, two active sites colocalize on each side of the tetramer, separated by ~25 Å (active sites A and D on one side, B and C on the other; Fig. 1*c*). The product of the first reduction could become the substrate in the adjacent catalytic site. The interface formed between the A and D (or B and C) subunits involves the C-terminus of one subunit positioned between the loop linking β5 to α5 and the C-terminus of the partner. This interface positions the side chain of Arg 287 in the active site of the partner subunit, which interacts with the substrate DHB through a bridging water (Fig. 2).

The active site interactions with DHB and NADPH

The catalytic center lies in a curved cleft, which extends for ~30 Å with a depth of 15 Å. DHB binds with the pterin sandwiched between Phe 113 and the nicotinamide by using all eight functional groups in hydrogen bond interactions, five of which are directly with the cofactor (Fig. 2). Such extensive interaction between substrate and nicotinamide is unique to PTR1 amongst the SDR family members. DHB is oriented with the site of the first reduction, the C7–N8 bond, near Asp 181 with N8 donating a hydrogen bond to Tyr 194 OH. The other side of the pterin, where the second reduction occurs at the C6–N5 bond, is directed out of the cleft. DHB N5 and O4 form hydrogen bonds with an ordered water; O4 also accepts a hydrogen bond from Arg 17.

Since a large part of the pterin binding site is formed by the nicotinamide, the substrate can only bind effectively after formation of the protein–cofactor complex. The pterin moiety, once positioned, effectively plugs the active site. Therefore, after catalysis the product has to vacate the active site before NADP+ can depart. Such an ordered, sequential mechanism is common in SDRs[8–11].

The cofactor adopts an extended conformation with the adenine *anti* and the nicotinamide *syn* with respect to their ribose groups. No restraints were imposed on sugar pucker. In each complex, the adenine ribose refined to an unusual C4′-*exo* conformation and the nicotinamide ribose to a more common C2′-*endo* pucker. The adenosine binding site is formed by the C-terminal regions of strands β1, β2 and β3; helix α4; and the loops linking β1 and β2 with the N-terminal regions of α1 and α2, respectively. The nicotinamide binds in a pocket formed by residues at the C-terminal ends of β5 and β6; its carboxamide hydrogen bonds to the main chain amide and carbonyl groups of Ser 227. Lys 198 binds and positions the cofactor with hydrogen bonds to the 2′- and 3′-OH groups of the nicotinamide ribose (Fig. 2).

The interaction between PTR1 and NADPH differs from other SDRs in two respects. First, most SDR family members carry a GXXXGXG (where X is any amino acid) motif involved in cofactor recognition[11], whereas Arg 17 in PTR1 replaces the second Gly residue. Arg 17 donates hydrogen bonds to the pyrophosphate of NADPH and to the O4 of DHB (Fig. 2); its contributing role in catalysis is described below. Second, PTR1 deviates from the established pattern for the determination of nucleotide (NADH *versus* NADPH) specificity in which two basic side chains interact directly with the 2′-phosphate of NADPH[11]. Although a sequence alignment (not shown) places Lys 16 and Arg 39 in the correct positions in PTR1, the side chains do not interact with the 2′-phosphate. Instead PTR1 confers specificity using the main chain of His 38, Arg 39 and Ser 40 to create a 2′-phosphate-binding pocket.

One active site, two reductions

Short-chain reductases catalyze the reduction of a C=O or C=N double bond. The common mechanism that has been proposed[10,11] involves a hydride transferred from NAD(P)H to the electrophilic carbon of the substrate bond. Following this is

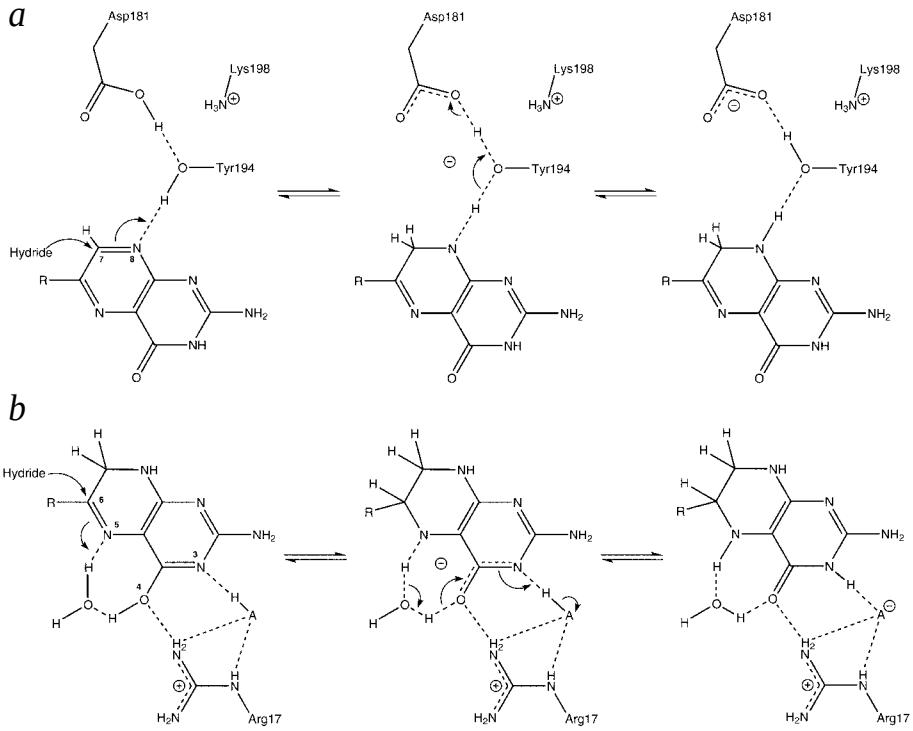

Fig. 3 The mechanism of PTR1. ***a***, The first step leading to the dihydro-form. Replacement of the catalytic triad Ser residue with Asp allows further delocalization of the negative charge of the transition state, leading to improved stabilization. ***b***, The second reduction to produce the tetrahydro-form. AH represents the acidic cofactor phosphate that interacts with N3 and A^-, the basic group.

addition of a proton in a reaction that involves a catalytic triad: a Tyr, a Lys and a (less well conserved) Ser residue. The Tyr residue (Tyr 194 in PTR1) hydrogen bonds to the nucleophilic center of the substrate bond, stabilizes the transition state and provides the proton transferred in the reaction. The Lys residue (Lys 198 in PTR1) may lower the pK_a of the tyrosine, stabilize the transition state by electrostatic interaction with the transient tyrosinate and function as the proton source for the tyrosine. In PTR1, a role for this Lys in proton transfer to the tyrosine is unlikely given that nearly 5 Å separates the OH of Tyr 194 from the NZ of Lys 198 and that the lysine ε-amino group is directed away from the tyrosine hydroxyl. The function of the third member of the catalytic triad, serine, is less well defined; it may help to stabilize the transition state and, in some cases, may play a role in proton relay. In PTR1, the residue corresponding to serine is Asp 181.

DHB participates in both reduction steps catalyzed by PTR1, first as product and then as substrate. We show that both reductions utilize the same substrate orientation. The pterin C7–N8 bond is correctly positioned for reduction by the SDR catalytic machinery, with C7 3.4 Å from the nicotinamide C4 (hydride donor) and N8 2.9 Å from the OH of Tyr 194 (Fig. 2). Therefore, the PTR1–$NADP^+$–DHB structure shows the pterin orientation corresponding to the product complex of the first reduction (Fig. 3*a*). This is further supported by the 2.4 Å resolution structure of a PTR1–$NADP^+$–biopterin complex (not shown), which has the orientation of biopterin virtually identical to that of DHB. For the second reduction (of the N5–C6 bond), the only binding mode that yields the correct chirality at C6 and maintains a suitable distance between C6 and the hydride donor is that observed in the PTR1–$NADP^+$–DHB complex. The distance (At 3.5 Å) between the nicotinamide C4 and pterin C6 is conducive to hydride transfer; however, an alternative proton donor for the second reduction is required. Mutagenesis studies show that Tyr 194 is required for the first reduction[12,13] but not the second[14], suggesting a catalytic triad-independent mechanism for that step.

Tyr 194 forms a hydrogen bond with N8 and is the proton donor in the first reduction. Asp 181 forms a hydrogen bond with Tyr194 OH but, unlike the analogous Ser residue in other SDRs, does not interact directly with the substrate. Mutagenesis of Asp 181 shows that PTR1 activity requires an acid in this position[14] and that the optimum pH for the reduction of biopterin is 4.7 (ref. 8). The decrease in activity above this pH likely corresponds to deprotonation of the solvent-accessible Asp 181. The comparison with the mentioned PTR1–$NADP^+$–biopterin complex also supports the participation of protonated Asp 181 in the reduction of oxidized pterins: in both structures, the distances between the substrate N8 and OH of Tyr 194 and between the OH of Tyr 194 and the OD2 of Asp181 indicate hydrogen bonding interactions. In the biopterin complex, the pterin can only accept a hydrogen bond from the OH of Tyr 194, which indicates that Asp 181 is protonated and donates a hydrogen bond to Tyr 194.

The second reduction proceeds in similar fashion to the first: the binding of NADPH is followed by substrate — for example, DHB — hydride transfer to C6 occurs, and finally N5 is protonated (Fig. 3*b*). The main difference between the two reduction steps is that the proton source is not Tyr 194 but a suitably positioned water molecule. An unactivated water may suffice as the proton donor; however, we propose that the pK_a is decreased by interaction with the acidic 4-hydroxy group of the enolized substrate. The enolization of the 4-keto function and the correct orientation of the resulting 4-OH is favored by interaction with the NADPH diphosphate and Arg 17. The cofactor phosphate may be a temporary acceptor for the N3 proton during enol formation (A^-/AH, Fig. 3*b*). Alternatively, the substrate N3 may retain the proton during catalysis. This mechanism is analogous to that of DHFR[15,16]; however, an Asp residue takes the role of the diphosphate, and a water replaces Arg 17. The Asp residue is not protonated during catalysis in DHFR[16].

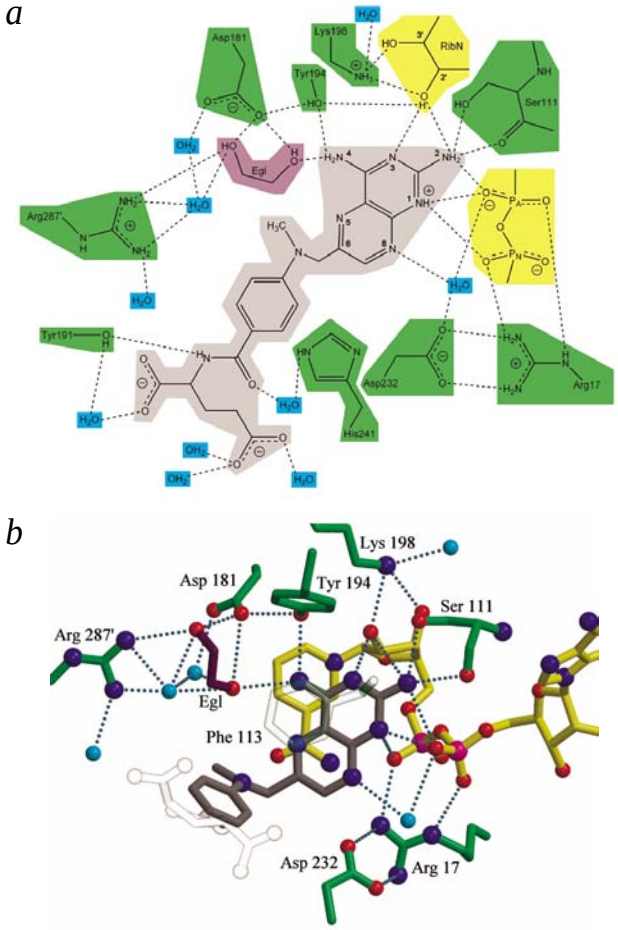

Fig. 4 The interactions of MTX with PTR1 and NADPH. ***a***, Schematic. ***b***, The three-dimensional arrangement. The same color coding as Fig. 2 is used, and, in addition, purple shading and the label 'Egl' identify ethylene glycol. The γ-glutamyl tail of MTX and Phe 113 are ghosted for clarity.

At the end of either reduction, the product leaves the active site to allow the exchange of $NADP^+$ for NADPH. We did not observe any significant structural changes in the NADPH and $NADP^+$ interactions with PTR1. Product elimination could be driven by the loss of aromaticity compared to substrate, leading to diminished affinity for the active site, and by electrostatic repulsion between the now positively charged nicotinamide and the protonated amino/imino groups of the pterin.

Substrate inhibition

For PTR1, dihydropterins but not oxidized pterins act as substrates and inhibitors[4,8]. Because both substrate types have similar geometries and bind in a similar orientation, it is remarkable that only one should display substrate inhibition. In pterin, N8 is a hydrogen bond acceptor but in dihydropterin, a donor. This suggests that pterins would preferentially bind to PTR1 when Tyr 194 offers a hydrogen bond to the active site — that is, when Asp 181 is protonated (Fig. 3*a*). Accordingly, dihydropterins would preferentially bind to 'deprotonated PTR1'.

When substrate encounters PTR1 that is not in the 'preferred' protonation state — for example, pterin with 'deprotonated PTR1' — it is likely that the unfavorable acceptor–acceptor interaction has only a minor influence on substrate binding when considering the numerous other advantageous interactions. As Asp 181 is solvent accessible independent of substrate binding, protonation of PTR1 could occur even after pterin binds and catalysis proceeds. Binding of a dihydropterin to 'protonated PTR1' in the established fashion would lead to an extremely unfavorable donor–donor contact with a hydrogen–hydrogen distance of <1.0 Å. The substrate may adopt a different (and nonproductive) orientation in the active site, thereby acting as an inhibitor. This explanation agrees with mutagenesis studies[14] that showed that a Y194F mutant of PTR1 has a higher specific activity towards DHF than wild type PTR1. We propose that this mutant mimics a permanently deprotonated PTR1, thereby alleviating substrate inhibition.

MTX Inhibition of PTR1

Similar to the DHB complex, the binding of MTX to PTR1–NADPH is dominated by interactions with the cofactor. There are five hydrogen bonds with the cofactor, and an ordered ethylene glycol, the cryoprotectant, binds in the active site, mimicking part of the water structure observed in the DHB complex (Fig. 4). However, the pteridine ring of MTX binds in a different orientation, rotated about the N2–N5 axis by 180°, relative to that observed for DHB (Fig. 4). This is reminiscent of MTX and folate binding to DHFR[17,18].

PTR1 is less susceptible to MTX inhibition than DHFR[5]. The interactions between MTX and PTR1–NADPH occur principally at the pterin end of the drug and involve direct hydrogen bonds with the cofactor. In contrast, when complexed with DHFR[19], all components of MTX form abundant protein–ligand interactions that result in tight binding. More important, there are specific and strong associations between the glutamyl tail of MTX and basic residues in DHFR. In PTR1, the 2,4-diaminopteridine is well defined in the crystal structure, but the *p*-aminobenzoyl (pABA) group and the glutamyl tail, which are directed away from the catalytic center towards the surface of the protein, are less so. The absence of molecular restraints and the availability of space in that area of the active site occupied by pABA and the glutamyl tail provide an explanation of the broad-spectrum activity of PTR1 (ref. 4). The binding mode of MTX also explains the sensitivity of PTR1 inhibition to substitutents on N2 or N4 of the 2,4-diaminopteridine scaffold and the tolerance for structural diversity of substituents at C6 of the scaffold[5].

Conclusions

PTR1 accomplishes two modes of reduction in a single active site. The first reduction, similar to that of other SDR family members, utilizes an Asp residue instead of a Ser to acquire a proton. The second reduction presents similarities with DHFR and provides an example of convergent evolution of mechanism. The architecture of PTR1 allows trypanosomatids to reduce and utilize a wide range of pterins acquired from the host or recycled, and provides the flexibility to balance salvage and recycling processes as required. A comparison with DHFR explains why PTR1 is relatively insensitive to MTX inhibition and why antifolate therapies have failed in the treatment of trypanosomatid infections. Any antifolate therapy targeting the bifunctional DHFR-TS of trypanosomatids must also target PTR1 to block the bypass and allow effective inhibition of essential folate metabolism. Tests of a spectrum of antifolates have provided encouragement for this supposition[5]. Therefore, it is necessary to develop two separate compounds inhibiting the individual enzymes or a single compound with good inhibitory properties against both. Accurate structures of PTR1–ligand complexes will

Table 1 Data collection, phasing and refinement statistics.

	SeMet λ_1 (peak)	SeMet λ_2 (inflection)	SeMet λ_3 (remote)	MTX complex	DHB complex
Wavelength (Å)	0.9795	0.9796	0.8860	0.8700	0.9326
Resolution range (Å)	19.96–2.80	19.96–2.80	19.50–2.50	30.00–1.75	27.77–2.20
Measurements	64,820	61,871	84,270	342,608	449,654
Unique reflections	13,461	11,935	17,507	59,475	62,471
Coverage overall (%)[1]	95.1	91.8	88.0	98.2	91.1
R_{sym} (%)[1]	4.7 (17.5)	4.4 (15.5)	4.1 (17.8)	4.5 (27.0)	7.7 (19.8)
R_{anom} (%)[1]	5.1	3.8	3.5		
R_{iso} (%)[1]	3.0		6.6		
Phasing power[2]	0.73 / 0.56		1.86 / 1.46		
Number of residues / solvents				525 / 481	1,047 / 434
R_{work}/R_{free}				19.6 / 24.4	19.8 / 22.7
R.m.s. deviations					
Bonds (Å)				0.015	0.014
Angles (°)				2.9	1.6
Wilson B / Average B (Å^2)				25.7 / 32.5	25.3 / 23.7

[1]Numbers in parenthesis refer to a high resolution bin of approximate width 0.1Å.
[2]Acentric / centric.

now aid further research directed towards the design and discovery of such inhibitors.

Methods

Crystallization and data collection. Recombinant *L. major* PTR1 ternary complexes and the selenomethionine (SeMet) derivative were obtained using established protocols[20]. Crystals of the PTR1–NADP$^+$–DHB complex are similar to those reported[20]; orthorhombic; with unit cell dimensions of a = 94.34, b = 103.80, c = 137.41 Å; and of space group $P2_12_12_1$ with a tetramer in the asymmetric unit. Another crystal form was obtained for the PTR1–NADPH–MTX complex and used for structure determination. Orthorhombic prisms were grown by vapor diffusion against 12% (v/v) polyethylene glycol monomethylether 5000, 100 mM sodium acetate, pH 5.5, and 100 mM calcium acetate. The space group is $P2_12_12$ with unit cell dimensions of a = 80.31, b = 80.80, c = 90.71 Å and two subunits per asymmetric unit.

All crystals were maintained at –173 °C during data collection (using glycerol or ethylene glycol as cryoprotectant). A SeMet derivative of the PTR1–NADPH–MTX complex (unit cell a = 80.64, b = 81.25, c = 89.45 Å) was used at BM14 ESRF. High-resolution data were subsequently measured on PX9.6 at SRS Daresbury, whereas data for the DHB complex were measured on ID14-EH2 ESRF. Data were processed (HKL suite[21]) then analyzed with CCP4 software[22] (Table 1).

Structure determination and refinements. Six Se positions were located[23] and used in a multiple isomorphous replacement approach to provide phases to 2.8 Å with a figure-of-merit of 0.59. Density modification[24] improved this to 0.72 at 2.1 Å (Table 1). The resulting map was interpreted using O[25] and refinement initiated using REFMAC[26]. The DHB complex was solved by molecular replacement (AMoRe[27]) with a model derived from the MTX complex. Rounds of model building/manipulation, solvent identification, and positional and B-factor refinement using CNS[28] or REFMAC[26] completed the refinements (Table 1). Poorly defined residues have either been omitted from the models or assigned zero occupancy. Figures were produced using MOLSCRIPT[29] and RASTER-3D[30].

Coordinates. Coordinates and structure factors have been deposited in the Protein Data Bank (accession codes 1E7W and 1E92 for MTX and DHB complexes, respectively).

Acknowledgments
We thank C. Bond, C. Frieden, D. Hall and A. Mehlert for discussions, and Daresbury and ESRF for support. Funded by the Wellcome Trust, BBSRC and N.I.H. grants.

Correspondence should be addressed to W.N.H. *email: w.n.hunter@dundee.ac.uk*

Received 4 January, 2001; accepted 27 March, 2001.

1. Bello, A.R., Nare, B., Freedman, D., Hardy, L. & Beverley, S.M. *Proc. Natl. Acad. Sci. USA* **91**, 11442–11446 (1994).
2. Kundig, C., Haimeur, A., Legare, D., Papadopoulou, B. & Ouellette, M. *EMBO J.* **18**, 2342–2351 (1999).
3. Nare, B., Hardy, L. & Beverley, S.M. *J. Biol. Chem.* **272**, 13883–13891 (1997).
4. Nare, B., Luba, J., Hardy, L. & Beverley, S.M. *Parasitology* **114**, S101–S110 (1997).
5. Hardy, L.W., Matthews, W., Nare, B. & Beverley, S.M. *Exp. Parasitol.* **87**, 158–170 (1997).
6. Beverley, S.M. *Annu. Rev. Microbiol.* **45**, 417–444 (1991).
7. Papadopoulou, B., Roy, G. & Ouellette, M. *EMBO J.* **11**, 3601–3608 (1992).
8. Luba, J. *et al. Biochemistry* **37**, 4093–4104 (1998).
9. Duax, W.L., Griffen, J.F. & Ghosh, D. *Curr. Opin. Struct. Biol.* **6**, 813–823 (1996).
10. Jörnvall, H. *et al. Biochemistry* **34**, 6003–6013 (1995).
11. Tanaka, N. *et al. Structure* **4**, 33–45 (1996).
12. Chang, C.-F., Bray, T. & Whiteley, J.M. *Arch. Biochem. Biophys.* **368**, 161–171 (1999).
13. Leblanc, E., Papadopoulou, B., Bernatchez, C. & Ouellette, M. *Eur. J. Biochem.* **251**, 768–777 (1998).
14. Luba, J. PhD Thesis, *Studies of Leishmania major pteridine reductase 1, a novel short chain dehydrogenase* (University of Massachusetts Medical School; 1999).
15. Blakley, R.L. *Adv. Enzymol. Relat. Areas Mol. Biol.* **70**, 23–102 (1995).
16. Casarotto, M.G., Basran, J., Badii, R., Sze, K.-H. & Roberts, G.C.K. *Biochemistry* **38**, 8038–8044 (1999).
17. Charlton, P.A., Young, D.W., Birdsall, B., Feeney, J. & Roberts, G.C.K. *J. Chem. Soc. Perkin Trans.* **191**, 1349–1353 (1985).
18. Birdsall, B. *et al. FEBS Lett* . **402**, 157–161 (1997).
19. Knighton, D.R. *et al. Nature Struct. Biol.* **1**, 186–194 (1994).
20. Gourley, D.G., Luba, J., Hardy, L.W., Beverley, S.M. & Hunter, W.N. *Acta Crystallogr. D* **55**, 1608–1610 (1999).
21. Otwinowski, Z. & Minor, W. *Methods Enzymol.* **276A**, 307–326 (1997).
22. Collaborative Computational Project Number 4. *Acta Crystallogr. D* **50**, 760–763 (1994).
23. Terwilliger, T.C. & Berendzen J. *Acta Crystallogr. D* **55,** 849–861 (1999).
24. Cowtan, K. *Joint CCP4 and ESF-EACBM Newsletter on Protein Crystallography*, **31**, 34–38 (1994).
25. Jones, T.A, Zou, J.Y. Cowtan, S.W. & Kjeldgaard, M. *Acta Crystallogr. A* **47**, 110–119 (1991).
26. Murshodov, G.N., Vagin, A.A. & Dodson, E.J. *Acta Crystallogr. D* **53**, 240–255 (1997).
27. Navaza, J. *Acta Crystallogr. A* **50**, 157–163 (1994).
28. Brünger, A.T. *et al. Acta Crystallogr. D* **54**, 905–921 (1998).
29. Kraulis, P.J. *J. Appl. Crystallogr.* **24**, 946–950 (1991).
30. Merritt, E.A. & Murphy, M.E.P. *Acta Crystallogr. D* **50**, 869–873 (1994).